

Phase Diagrams of the Harper Map and the Golden Staircase

P. Castelo Ferreira^{1*}, F. P. Mancini^{1†} and M. H. R. Tragtenberg^{1,2‡}

¹*Department of Physics, University of Oxford, 1 Keble Road, Oxford, OX1 3NP, UK*

²*Depto. de Física, Univ. Fed. de Santa Catarina, Florianópolis, SC, Brazil, CEP 88040-900*
(November 5, 2018)

We present phase diagrams of the Harper map, which is equivalent to the problem of Bloch electrons in a uniform magnetic field (Azbel-Hofstadter model). We consider the cases where the magnetic flux ω assumes either the continued fraction approximations towards the golden mean or the golden mean itself. The phase diagrams for rational values of ω show a finite number of Arnol'd tongues of localized electronic states with rational winding numbers and regions of extended phases in between them. For the particular case of $\omega = \frac{\sqrt{5}-1}{2}$, we find an infinite number of Arnol'd tongues of localized phases with extended phases in between. In this case, the study of the winding number gives rise to a Golden Staircase, where the plateaux represent localized phases with winding numbers equal to sums of powers of the golden mean. We also present evidence of the existence of an infinite number of strange nonchaotic attractors for $\epsilon = 1$ in points analogous to critical points in the pressure-temperature phase diagram of the water. [OUTP-00-07S]

Pacs: 03.65.Sq, 05.45.-a, 71.30.+h Keywords: Azbel-Hofstadter, Harper equation, Harper map, phase transitions, strange nonchaotic attractors, fractal, golden staircase

The Schrödinger equation for one electron in a two-dimension periodic lattice on a uniform magnetic field, in the tight binding approximation and Landau gauge, is known as the Azbel-Hofstadter problem [1,2]. The discretized version of this model is the Harper equation [3]

$$\psi_{n+1} + \psi_{n-1} + 2\epsilon \cos[2\pi(\phi_0 + \omega n)]\psi_n = E\psi_n \quad (1)$$

where ψ_n is the discretized wave function, ϵ is the lattice potential strength and ω is the magnetic flux per unit cell in units of the quantum flux (for reviews see [4,5]). Under the transformation of variables $x_n = \psi_{n-1}/\psi_n$ we obtain the Harper map [6]

$$x_{n+1} = \frac{-1}{x_n - E + 2\epsilon \cos(2\pi\phi_n)}, \quad (2)$$

where $\phi_n = (\phi_0 + \omega n) \bmod 1$. We take $\phi \in [0, 1[$ due to the cosine periodicity.

The Lyapunov exponent related to the ϕ dynamics is 0 and the one concerning the variable x is given by

$$\lambda = \lim_{N \rightarrow \infty} \frac{1}{N} \sum_{n=0}^N y_n, \quad (3)$$

where

$$y_n = \log \frac{\partial x_{n+1}}{\partial x_n} = \log x_{n+1}^2. \quad (4)$$

Prasad *et al.* [7] have studied in detail the Localized-Extended transition for $\omega = \omega^* = (\sqrt{5}-1)/2$ (golden mean), $\epsilon = 1$ and $E = 0, \pm 2.597 \dots$ (center and band edges of the spectrum). They found interesting connections between strange nonchaotic attractors (SNA) [8] and localized-extended transition in the electronic wave function. We extend their analysis for all values of E and other typical rational values of ω .

Our study is based on the analysis of the Lyapunov exponent λ as a function of the parameters ϵ, E and ω . Aubry and André [9] proved that the Lyapunov exponent λ is proportional to the localization length γ :

$$\lambda = \lim_{N \rightarrow \infty} \frac{1}{N} \log \left(\frac{\psi_0}{\psi_N} \right)^2 = -2\gamma. \quad (5)$$

For the Harper map $\lambda \leq 0$. If $\lambda = 0$, the phase is Extended (E), but for $\lambda < 0$ the phase is Localized (L).

All the characteristics discussed here are numerical results. We start our analysis of the Harper map by discussing the phase diagrams $\epsilon \times E$ for successive approximations $\omega_m = F_{m-1}/F_m$ to the golden mean, where $F_0 = F_1 = 1$ and $F_m = F_{m-1} + F_{m-2}$ (Fibonacci sequence). In this paper we show the results for $\omega = 5/8$ and $8/13$, which display the essential features of the phase diagrams for other orders of approximation for the golden mean. Then, we exhibit the phase diagram for $\omega = \omega^*$.

The $\epsilon \times E$ phase diagrams are symmetric by reflection in relation to the axes $E = 0$ and $\epsilon = 0$. Then, we will refer only to their first quadrant. For a given ω_m , there are $F_{m-1}(F_{m-1} - 1)$ connected regions of L(E) phases. The particular stability limits of each phase depend only on the value of the initial condition for the variable ϕ , namely ϕ_0 . This behavior gives rise to co-stability regions, where more than one configuration is stable. The stability limits for different ϕ_0 are invariant under the transformation $\phi_0 \rightarrow \phi_0 + 1/F_m$.

Fig. 1 shows the phase diagram for $\omega = 5/8$. We observe a *finite number of Arnol'd tongues*, a new feature in phase diagrams, as far as we know. The white regions (L phases) are labelled by winding numbers [10] $\Omega = p/F_m$, where $p = 0, 1, 2, \dots, F_m - 2$. In the lighter shaded regions we can find either L or E configurations, *depending on the value of ϕ_0* . In the darkest shaded regions there are E phases. The dashed curves represent the stability

limits of the Localized phases for $\phi_0 = 0$, whereas the continuous lines represent these limits for $\phi_0 = 1/16$. In the $E = 0$ axis there are two cases. For even F_m , there is an E phase for $0 \leq \epsilon \leq \epsilon_1 < 1$; for $\epsilon_1 < \epsilon < \epsilon_2$ there is an E/L co-stability region. For $\epsilon > \epsilon_2$ there is a L phase. For odd F_m , there is an E phase if $0 \leq \epsilon \leq 1$ and a L phase for $\epsilon > 1$. In the limit $m \rightarrow \infty$, ϵ_1 and $\epsilon_2 \rightarrow 1$, and the behavior for odd and even F_m become the same [7].

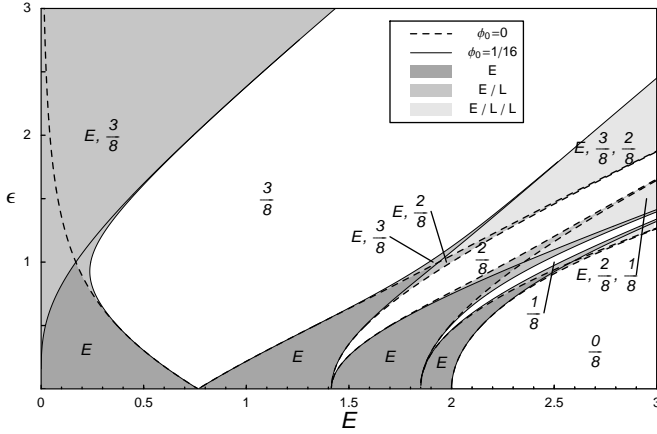


FIG. 1. Phase diagram for $\omega = 5/8$. The labels represent the winding numbers Ω of Localized phases. In the white regions there are Localized phases, in lighter shaded regions there are co-stability of L and E configurations and in the darkest shaded regions there are Extended phases.

The attractors of the Harper map corresponding to L phases, for a given ω_m , are F_m - *cycles*, i.e., cycles with period F_m . In the particular case of Fig. 1, they are 8-cycles. The configurations corresponding to Extended phases are unidimensional. For $\omega = 5/8$, typical E and L configurations are represented in Fig. 2.

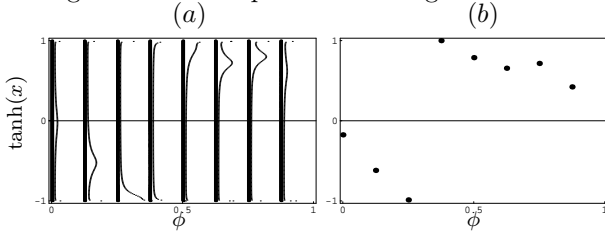


FIG. 2. E and L configurations for $\omega = 5/8$ and $\epsilon = 0.5$. The E-L transition takes place at $E = 0.370773\dots$ (a) Extended phase, $E = 0.34$; the thick lines represent the configuration and the thin lines the probability distribution of the iterations. (b) Localized phase, $E = 0.39$; this attractor has winding number $\Omega = 3/8$.

In general, for a given $\omega_m = F_{m-1}/F_m$, the configuration of an Extended phase is made up by F_m vertical lines in the plane $\tanh(x) \times \phi$. The E-L transition occurs when the most visited points in the unidimensional E phase turn to be a F_m - *cycle* of the Localized phase, as the energy and/or ϵ varies.

The Localized phases within the white regions in Fig. 1 are actually *co-stability regions*. There are many stable F_m - *cycles* within each Arnol'd tongue, all of them with

the same winding number. Fig. 3 represents the Lyapunov exponent λ as a function of the energy, for three different values of ϕ_0 . We see in Fig. 3a the co-stability of an Extended configuration with two Localized attractors. In Fig. 3b we see three stable attractors, all with winding number $\Omega = 3/8$.

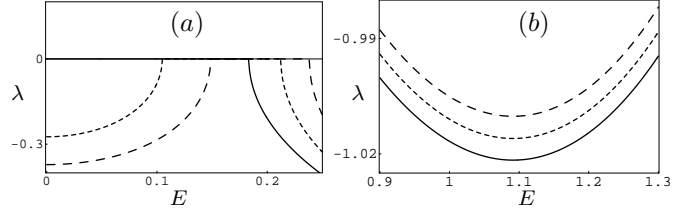


FIG. 3. The Lyapunov exponent λ vs. E for $\omega = 5/8$, $\epsilon = 0.95$ and for $\phi_0 = 0$ (continuous line), $\phi_0 = 1/32$ (dashed line), $\phi_0 = 1/16$ (long dashed line). (a) shows co-stability between Extended and Localized configurations; (b) shows co-stability between different Localized attractors.

The winding number changes with the energy. Fig. 4 shows the variation of Ω as a function of E for $\omega = 5/8$. We see plateaux with winding numbers $3/8$, $2/8$, $1/8$ and $0/8$, which represent Localized phases.

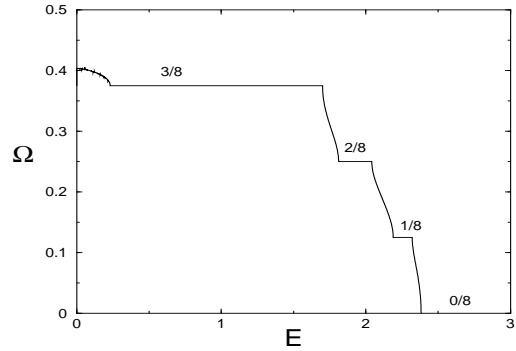


FIG. 4. Typical staircase for rational values of ω , representing the winding number Ω as a function of the energy. Here, $\omega = 5/8$, $\epsilon = 0.8$ and $\phi_0 = 5/8$. There are four plateaux corresponding to the winding numbers $3/8$, $2/8$, $1/8$ and $0/8$. The winding number for $E = 0$ is also $3/8$. These plateaux are connected through continuous lines, representing the Extended configurations.

The next approximant of ω towards ω^* is $8/13$. The number of Arnol'd tongues, as well as connected Extended regions have increased. The stability limits for $\phi_0 = 0$ are plotted in Fig. 5, but the full phase diagram must take into account all initial conditions. Nevertheless, the structure of tongues with pure Localized phases surrounded by L-E co-stability regions is the same as in Fig. 1. The winding numbers are labelling the Localized regions, made up by 13-cycles.

The number of phase transition lines increases as we approach ω^* , becoming infinite in the limit $\omega \rightarrow \omega^*$. The phase diagram of the Harper map for $\omega = \omega^*$ is in Fig. 6. The labels within the Arnol'd tongues are the winding numbers of the Localized phases.

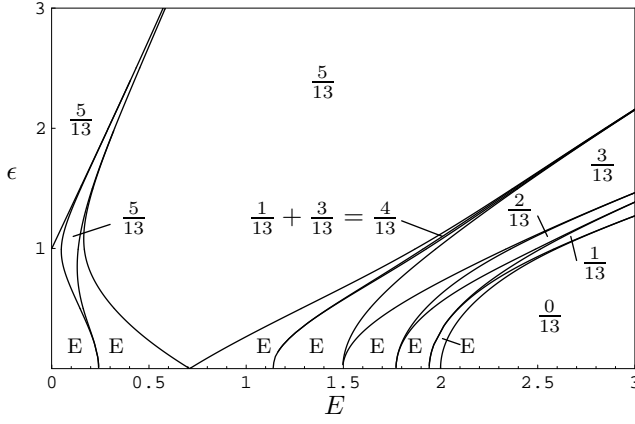


FIG. 5. Stability limits of the Localized and Extended phases for $\omega = 8/13$, $\phi_0 = 0$.

The L-E transitions do not depend on the initial condition, then there are no co-stability regions. There is only one attractor for a given point inside a L phase, as can be checked by calculating the Lyapunov exponent. This calculation also shows the fractal character of this phase diagram [11].

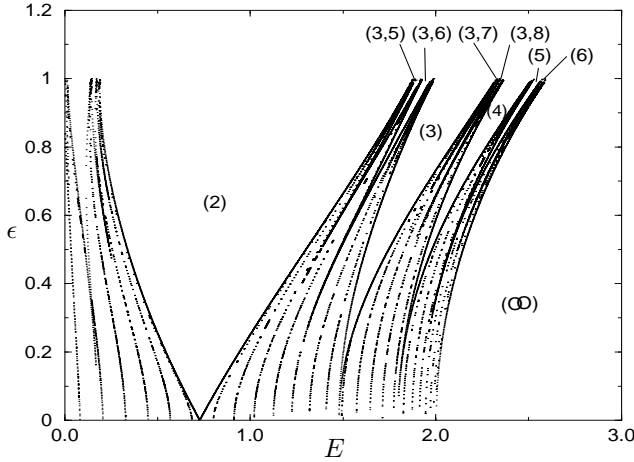


FIG. 6. Phase diagram of the Harper map for $\omega = \omega^*$. The labels of the L phases are their winding numbers. The L-E transitions, represented as the boundaries of the L phases, end in SNAs for $\epsilon = 1$. Unlike the phase diagrams for rational ω , there are no co-stability regions and within each Arnol'd tongue there is only one attractor. The tongues to the left of the largest has variable winding number. Here we define $(k_1, k_2, k_3) \equiv \omega^{*k_1} + \omega^{*k_2} + \omega^{*k_3}$.

From now on a winding number given by a sum of powers of ω^* , say $\omega^{*k_1} + \omega^{*k_2} + \omega^{*k_3}$, will be represented by (k_1, k_2, k_3) .

In the case of Localized phases, the winding numbers for $\omega = \omega^*$ are limit values of those for $\omega_m = F_{m-1}/F_m$. In general, the phase with winding number $\Omega = \omega^{*k} = (k)$ (k integer) is the limit of the phases with $\Omega = F_{m-k}/F_m$, when $m \rightarrow \infty$. Moreover, the L-E phase transitions end at the line $\epsilon = 1$. Their endpoints have $\lambda = 0$ and are strange nonchaotic attractors like the one in $(\epsilon, E) = (1, 0)$, thoroughly analyzed in reference [7].

Therefore, there is evidence of the occurrence of an infinite number of SNAs in this phase diagram. One of them is shown in Fig. 7.

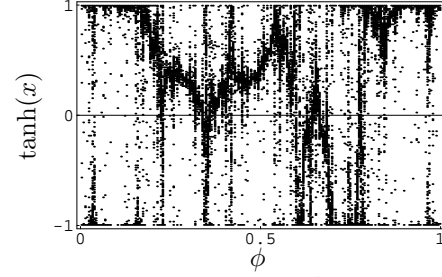


FIG. 7. Phase portrait of the SNA for $\omega = \omega^*$ and $\epsilon = 1$ at $E = 2.3447775 \dots$, the endpoint of the left boundary of the Localized phase with winding number ω^{*4} in Fig. 6.

For $\epsilon > 1$ all Lyapunov exponents become negative although they maintain their *bumpy* structure (see Fig. 8). This means that the transition between different L regions is smooth without crossing an E region. This resembles the liquid-vapor phase transition of the water. Above the critical point the change between liquid and vapor is smooth.

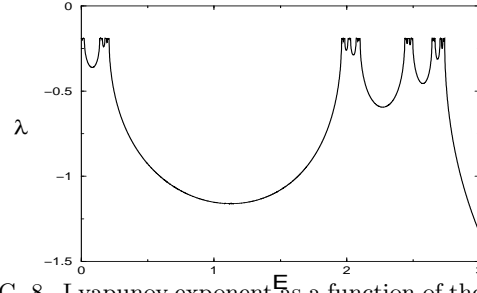


FIG. 8. Lyapunov exponent λ as a function of the energy, for $\epsilon = 1.1$ and $\omega = \omega^*$. The L phases occupy all the line, since $\lambda < 0$.

The typical E and L attractors are also different for $\omega = \omega^*$. In this case, the L-E transition is between a unidimensional and a two-dimensional attractor, as displayed in Fig. 9. The change in the energy and/or ϵ can cause a spread in the unidimensional L attractor towards a two-dimensional E phase, in the plane $\tanh(x) \times \phi$.

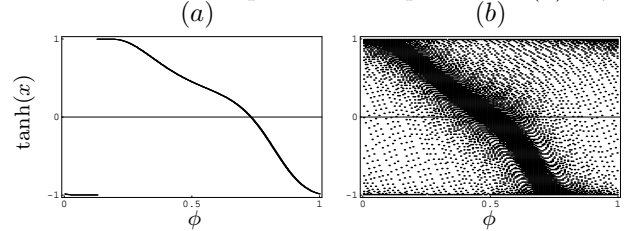


FIG. 9. Typical Localized and Extended configurations for $\omega = \omega^*$ and $\epsilon = 0.2$. (a) $E = 0.938$. (b) $E = 0.94$. The locus of the L-E transition is $E = 0.9391 \dots$

One of the most original features of the phase diagram for $\omega = \omega^*$ is the *irrationality of the winding numbers of the Localized phases within the Arnol'd tongues*. They are sums of powers of the golden mean. This is the first phase

diagram to show it, as far as we know. Starting from the left to the right, the largest phases have winding numbers such that $\Omega = \omega^{*j}$, where $j = 2, 3, 4, \dots, \infty$. The plot of Ω vs. energy for $\epsilon = 0.8$ shows a number of plateaux, corresponding to L phases. We name it **Golden Staircase** (see Fig. 10) and its structure is completely different from the Farey tree observed in many modulated and dynamical systems [12].

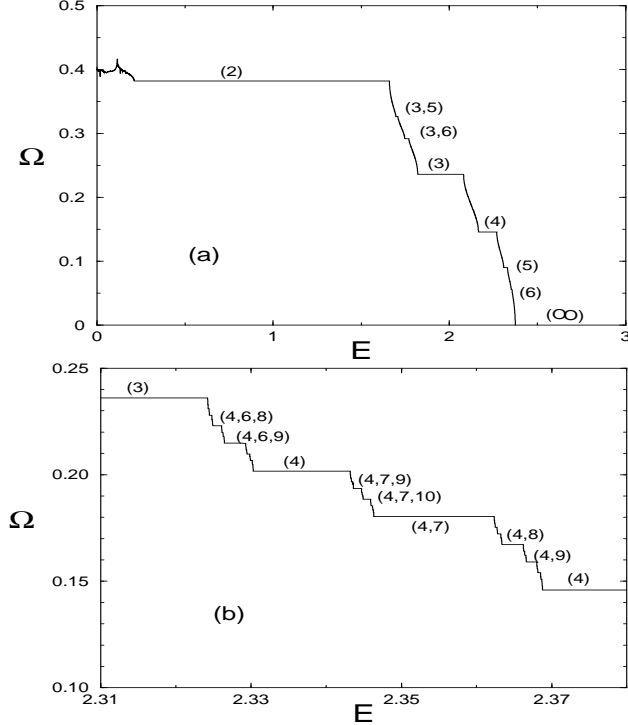


FIG. 10. (a) Winding number as a function of energy, for $\omega = \omega^*$ and $\epsilon = 0.8$. The plateaux correspond to L phases and their winding numbers are displayed. They are sums of powers of the golden mean. Between two plateaux there are other sets of plateaux, displaying a fractal structure. (b) Detail of the golden staircase for $\epsilon = 1$.

There is an order beneath the irrational labels of the L phases. Firstly, the main sequence of integer powers of the golden mean (k), for $k = 2, 3, 4, \dots$ occurs in a similar way between two elements of the same sequence. For example, take $k = 3$ and $k = 4$. These labels can be rewritten as $(3) = (4, 5)$ and $(4) = (4, \infty)$. Between them there are the winding numbers $(4, j)$, for $j = 6, 7, 8, \dots$. Secondly, given two neighboring tongues labelled by, say, (k) and $(k + 1)$ there is a rule to find out which are the two largest tongues between them. For example take the two largest tongues between (3) and (4) : $(4, 6)$ and $(4, 7)$. They correspond to the lowest powers of ω^* to be summed up to (4) . It is now easy to go one step down in the hierarchy; take the powers $(4, 6)$ and $(4, 7)$, which can be rewritten respectively, as $(4, 7, 8)$ and $(4, 7, \infty)$. Between them we find the winding numbers $(4, 7, j)$, for $j = 9, 10, 11, \dots$, where $(4, 7, 9)$ and $(4, 7, 10)$ are connected to the largest tongues. The other steps can be deduced following the same reasoning.

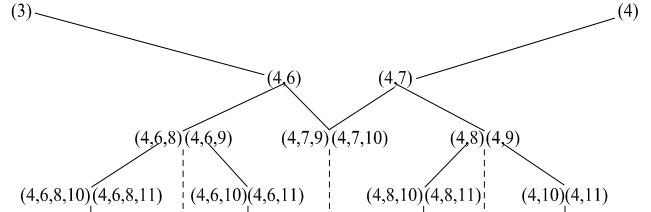


FIG. 11. Partial hierarchy of the L phases.

We conjecture that the lock-in of phases with irrational winding numbers should be a common feature for other irrational values of ω for the Harper map [13]. Besides, the structure of the diagram Ω vs. energy should resemble the one of the Golden Staircase.

In this letter we have presented phase diagrams for the Harper map for $\omega = 5/8, 8/13$ and ω^* . We described in detail the occurrence of finite or infinite number of Arnol'd tongues, strange nonchaotic attractors and the L-E transition in each case. We also reported the occurrence of co-stability regions and the peculiar structure of the staircases representing the winding number.

The study of the density of states with irrational winding numbers, following Thouless [14] will be subject of forthcoming publication.

The work of PCF is supported by PRAXIS XXI/BD/11461/97 grant from FCT (Portugal). The work of FPM is supported by EPSRC studentship 97304299 and by Fondazione A. Della Riccia. MHRT thanks O. Kinouchi for helpful discussions.

* pcastelo@thphys.ox.ac.uk, corresponding author

† mancini@thphys.ox.ac.uk

‡ marcelo@thphys.ox.ac.uk

- [1] M. Ya. Azbel, Sov. Phys. JETP **19**, 634 (1964).
- [2] D. R. Hofstadter, Phys. Rev. **B14**, 2239 (1976).
- [3] P. G. Harper, Proc. Phys. Soc. London **A68**, 874 (1955).
- [4] B. Souillard, Phys. Rep. **103**, 41 (1984).
- [5] J. B. Sokoloff, Phys. Rep. **126**, 189 (1985).
- [6] J. A. Ketoja and I. I. Satija, Physica **D109**, 70 (1997).
- [7] A. Prasad, R. Ramaswamy, I. I. Satija and N. Shah, Phys. Rev. Lett. **83**, 4530 (1999).
- [8] C. Grebogi, E. Ott, S. Pelikan and J. A. Yorke, Physica **D 13**, 251 (1984).
- [9] S. Aubry and G. André, Ann. Israel Phys. Soc. **3**, 133 (1980).
- [10] We define winding number as $\Omega = \lim_{N \rightarrow \infty} S/(2N)$, where S is the number of times the variable x changes sign during N iterations.
- [11] J. Bellissard and B. Simon, J. Funct. Anal. **48**, 408 (1982).
- [12] O. Kinouchi and M.H.R. Tragtenberg, Int. J. of Bifurcation and Chaos **6**, 2343 (1996).
- [13] S. Y. Jitomirskaya and Y. Last, Commun. Math. Phys. **195**, 1 (1998).
- [14] D Thouless, J. Phys. C **5**, 77 (1972).